

Dark energy constraints from joint analysis of standard rulers and standard candles

Marek Biesiada^{1,2}, Beata Malec² and Aleksandra Piórkowska¹

¹ Department of Astrophysics and Cosmology, Institute of Physics, University of Silesia, Uniwersytecka 4, 40-007 Katowice, Poland; biesiada@us.edu.pl

² Copernicus Center for Interdisciplinary Studies, Gronostajowa 3, 30-387 Cracow, Poland

Received 2011 January 9; accepted 2011 February 2

Abstract We performed joint analysis of five cosmological models invoked to explain the accelerating expansion of the Universe. We used the data from strong gravitational lensing systems, locations of cosmic microwave background acoustic peaks and baryon acoustic oscillation data in combination with supernova Ia data (Union2 compilation). The observables we used came from both standard rulers and standard candles, so they had different parameter degeneracies and different restrictive powers in the parameter spaces of cosmological models. The best fits we obtained for the model parameters in joint analysis turned out to prefer cases effectively equivalent to the Λ CDM model. They were also in agreement with other combined studies performed by other authors on different sets of diagnostic probes. Information theoretic methods used to assess which model is most supported by the data lead to the conclusion that the concordance model Λ CDM is clearly preferred in joint analysis. The quintessence (both having constant or time varying equation of state) and Chaplygin gas get considerably less support from the data while the brane world (DGP) scenario is practically ruled out.

Key words: cosmology: observations — cosmological parameters — gravitational lensing — supernovae

1 INTRODUCTION

One of the most important issues in modern cosmology is the problem of the currently accelerating expansion of the Universe as inferred from the SNIa Hubble diagram (Perlmutter et al. 1999; Riess et al. 1998, 2004, 2007; Astier et al. 2006; Wood-Vasey et al. 2007; Kowalski et al. 2008; Hicken et al. 2009; Kessler et al. 2009; Amanullah et al. 2010) and supported by other independent studies including: cosmic microwave background radiation (CMBR) anisotropies (Hinshaw et al. 2009; Komatsu et al. 2009) and baryon acoustic oscillations imprinted in the large scale structure power spectrum (Eisenstein & Hu 1999; Eisenstein et al. 2005; Cole et al. 2005; Hütsi 2006a,b; Percival et al. 2007).

The explanation of this phenomenon is far from obvious and, broadly speaking, involves either invoking an unknown exotic (with negative net pressure) material component (so called “dark energy”) or modification of gravity at cosmological scales. Lacking clear theoretical guidance, we are left with the phenomenological approach based on upgrading observational fits of quantities which

parametrize the unknown (such as density parameters or coefficients in the cosmic equation of state) and seeking coherence among alternative tests and techniques.

In this spirit, we performed a joint analysis of various dark energy models using the data from supernovae, CMBR acoustic peaks, baryon acoustic oscillations (BAO) and strong lensing systems. These different tests will be called diagnostics for short. Part of the diagnostics makes use of the angular diameter distance and part of them uses the luminosity distance. These are two distance concepts which, although theoretically related to each other, clearly have different systematic uncertainties and different parameter degeneracies. Hence their joint analysis is more restrictive in the parameter space.

The next section describes these diagnostics and the data sets used. Section 3 presents cosmological scenarios tested and the results obtained. In Section 4, we pose the question which model is the best supported by combining evidence from the data and attempt to answer it with information-theoretic criteria. The final section contains the conclusions.

2 DATA SETS AND DIAGNOSTIC TOOLS

The main paradigm of modern cosmology is that the geometry of the Universe can be described as one of three possible Friedman-Robertson-Walker (FRW) solutions to the Einstein equations representing homogeneous and isotropic spacetime. Currently there exists strong evidence, coming from independent and precise experiments, that the Universe is spatially flat. For example, a combined analysis of WMAP5, BAO and supernova data (Hinshaw et al. 2009) gives $\Omega_{\text{tot}} = 1.0050_{-0.0061}^{+0.0060}$. Hence we will assume the flat ($k = 0$) FRW model from now on. The only gravitational degree of freedom is the scale factor $a(t)$ depending on cosmic time t and which is responsible for temporal changes of spatial length-scales (known as cosmic expansion). In particular, there is a unique correspondence between $a(t)$ and redshift z which is an observable quantity. By virtue of the Einstein equations, the expansion rate $H = \frac{\dot{a}}{a}$ is determined by some set of parameters like present expansion rate H_0 , present density of (pressureless) matter Ω_m , radiation Ω_r or any other material component Ω_x (if considered) and the equation of state parameter w (assuming a hydrodynamical energy momentum tensor using the $p = w\rho$ relation). We will use a shorthand notation of \mathbf{p} for such parameters. Their full specification will be given in Section 3, which presents the models tested. Technically speaking, testing cosmological models means determining parameters \mathbf{p} .

It is quite obvious that one very direct approach could be to test the distance – redshift relation $D(z)$ whenever there is the possibility to determine distances and redshifts independently. However, as a consequence of the assumed non-euclidean geometry, one distinguishes three types of distances in cosmology:

(i) comoving distance

$$r(z; \mathbf{p}) = c \int_0^z \frac{dz'}{H(z'; \mathbf{p})} = \frac{c}{H_0} \tilde{r}(z; \mathbf{p}), \quad (1)$$

where $\tilde{r}(z)$ denotes a reduced (dimensionless) comoving distance, i.e. a comoving distance expressed as a fraction of the Hubble horizon $d_H = c/H_0$,

(ii) angular diameter distance

$$D_A(z; \mathbf{p}) = \frac{1}{1+z} r(z; \mathbf{p}), \quad (2)$$

(iii) luminosity distance

$$D_L(z; \mathbf{p}) = (1+z)r(z; \mathbf{p}). \quad (3)$$

Angular diameter distance can be used as a standard ruler for objects whose size is known a priori. It is also used in gravitational lensing theory (because gravitational lensing deals with light

deflection which is essentially connected with angles). The luminosity distance is a measure invoked while using standard candles (in a cosmological context: SNIa or gamma ray bursts). Both distance measures are related to each other by a $(1+z)^2$ factor (see above) which is known as the Etherington reciprocity relation.

2.1 Standard Rulers

2.1.1 Strong lensing systems

Strong gravitational lensing occurs whenever the source, the lens and observer are so well aligned that the observer–source direction lies inside the so-called Einstein ring of the lens. In a cosmological context, the source is most often a quasar with a (usually elliptical) galaxy acting as the lens. Strong lensing reveals itself as multiple images of the source. The image separations in the system depend on angular-diameter distances to the lens and to the source, which in turn are determined by background cosmology. This opens a possibility to constraining the cosmological model provided that we have good knowledge of the lens model. Fortunately, there is growing evidence for a homologous structure of elliptical galaxies (Treu et al. 2006a,b; Koopmans et al. 2006, 2009). In particular, it was shown in Koopmans et al. (2009) that inside one effective radius, massive elliptical galaxies are kinematically indistinguishable from an isothermal ellipsoid.

The Einstein radius in an Singular Isothermal Sphere (SIS) lens (or its Singular Isothermal Ellipsoid (SIE) equivalent)

$$\theta_E = 4\pi \frac{\sigma_{\text{SIS}}^2}{c^2} \frac{D_{\text{ls}}}{D_s}, \quad (4)$$

depends on the cosmological model through the ratio of (angular-diameter) distances between lens and source and between observer and source. Then, if one knows the Einstein radius θ_E (from image astrometry) and stellar velocity dispersion σ_{SIS} (from central velocity dispersion σ_0 obtained from spectroscopy) one can use them to test the background cosmology.

Starting with the Lens Structure and Dynamics (LSD) survey and the more recent SLACS survey (Sloan Lens ACS Survey ¹) spectroscopic data, the central parts of lens galaxies became available allowing researchers to assess their central velocity dispersions. In practice, central velocity dispersion σ_0 is estimated from the velocity dispersion within $R_e/8$ where R_e is the effective optical radius. Detailed discussion of this issue can be found in Treu et al. (2006) and Grillo et al. (2008), where the arguments in favor of using σ_0 to represent σ_{SIS} are presented.

This method is independent of the Hubble constant's value (which gets canceled in the distance ratio) and is not affected by dust absorption or source evolutionary effects. This aspect was discussed in (Biesiada 2006) and also later in Grillo et al. (2008). In a recent paper (Biesiada et al. 2010), the dark energy equation of state (in the Chevalier-Polarski-Linder (CPL) parametrization) was estimated using a sample of strong lenses. The present paper extends it substantially both by considering more dark energy scenarios and by analyzing lenses jointly with other probes.

In the method used in this paper, the cosmological model enters not through a distance measure directly, but rather through a distance ratio

$$\mathcal{D}^{\text{th}}(z_l, z_s; \mathbf{p}) = \frac{D_s(\mathbf{p})}{D_{\text{ls}}(\mathbf{p})} = \frac{\int_0^{z_s} \frac{dz'}{h(z'; \mathbf{p})}}{\int_{z_l}^{z_s} \frac{dz'}{h(z'; \mathbf{p})}}, \quad (5)$$

and its respective observable counterpart reads

$$\mathcal{D}^{\text{obs}} = \frac{4\pi\sigma_0^2}{c^2\theta_E}.$$

¹ <http://www.slacs.org/>

Cosmological model parameters (coefficients in the equation of state) are estimated by minimizing the chi-square

$$\chi^2(\mathbf{p}) = \sum_i \frac{(\mathcal{D}_i^{\text{obs}} - \mathcal{D}_i^{\text{th}}(\mathbf{p}))^2}{\sigma_{\mathcal{D},i}^2}, \quad (6)$$

where the sum is over the sample and $\sigma_{\mathcal{D},i}^2$ denotes the variance of \mathcal{D}^{obs} (contextual use of the same symbol for variances and velocity dispersions should not lead to confusion). In calculating $\sigma_{\mathcal{D}}$, we assumed that only velocity dispersion errors contribute and the Einstein radii are determined accurately.

We used a combined sample of $n = 20$ strong lensing systems with good spectroscopic measurements of central dispersions from the SLACS and LSD surveys (essentially the same sample as used in Grillo et al. 2008). Original data concerning the SLACS sample came from Treu et al. (2006a, b). Data concerning LSD lenses are taken after Treu & Koopmans (2004); Koopmans & Treu (2002, 2003).

The sample is summarized in table 1 of Biesiada et al. (2010) where one can find the source and lens redshifts, Einstein ring diameters and central velocity dispersions. Here we just list the names of lensing systems considered. From the SLACS survey are: SDSS J0037–0942, J0216–0813, J0737+3216, J0912+0029, J0956+5100, J0959+0410, J1250+0523, J1330–0148, J1402+6321, J1420+6019, J1627–0053, J1630+4520, J2300+0022, J2303+1422, and J2321–0939 and from the LSD Survey are: Q0047–2808, CFRS03.1077, HST 14176, HST 15433, and MG 2016.

2.1.2 CMBR

Since the discovery of acoustic peaks in the power spectrum of the CMBR, it became clear that the measured angular scale of the first acoustic peak, given by $\vartheta_A = \frac{r_s(z_{\text{lss}})}{D_A(z_{\text{lss}})}$ where $r_s(z_{\text{lss}})$ is the comoving size of the sound horizon at the last scattering surface and $D_A(z_{\text{lss}})$ is the angular diameter distance to the last scattering surface, provided us with a very useful tool for testing cosmological models. The size of the sound horizon serves here as a standard ruler. In practice, one uses the scaled distance to the last scattering surface (at redshift z_{lss}) in the form of the so-called shift parameter (see e.g. Doran & Lilley 2002; Page et al. 2003 or most recently Shafieloo et al. 2009) $R(\mathbf{p}) = \sqrt{\Omega_m} \int_0^{z_{\text{lss}}} \frac{dz}{h(z;\mathbf{p})}$, where Ω_m is the present day matter density and $h(z)$ is the dimensionless (i.e. with H_0 factored out) expansion rate which depends on the cosmological model (through parameters \mathbf{p}). The first results on the R shift-parameter came from WMAP’s 3-year results (Spergel et al. 2007) and were confirmed later by WMAP’s 5-year data. We used the most recent result from WMAP7 (Komatsu et al. 2011) which is $R(\mathbf{p}) = 1.725 \pm 0.018$.

For comparison between theory and observations, we will use the chi-square function

$$\chi_{\text{CMB}}^2(\mathbf{p}) = \frac{[R(\mathbf{p}) - 1.725]^2}{0.018^2},$$

i.e. just “one data point” for joint analysis.

2.1.3 BAO

BAO are the pressure waves in the photon-baryon plasma of the early universe caused by dark matter overdensities. Besides producing the acoustic peaks of the CMBR, they reveal themselves in clustering properties of galaxies – as a bump in the two-point correlation function. The large-scale correlation function of luminous red galaxies in the Sloan Digital Sky Survey (Eisenstein et al. 2005) is a combination of the correlations measured in the radial (redshift space) and the transverse (angular space) direction (it is similar to the idea of the so called Alcock & Paczynski 1979 test).

Thus, the relevant distance measure is the so-called dilation scale, $D_V(z; \mathbf{p}) = [(1 + z)^2 D_A(z; \mathbf{p})^2 cz/H(z; \mathbf{p})]^{1/3}$ at the typical redshift of the galaxy sample, $z = 0.35$. The absolute scale of the BAO is given by the sound horizon at the last scattering surface (standard ruler). Then the dimensionless combination

$$A(z; \mathbf{p}) = D_V(z; \mathbf{p}) \sqrt{\Omega_m H_0^2 / cz} \quad (7)$$

is an observable quantity, well constrained by the data at $z = 0.35$. Its most recent value is (Reid et al. 2010)

$$A(0.35) = 0.493 \pm 0.017.$$

We will use this value as a diagnostic tool in the joint analysis. A convenient form of $A(z = 0.35; \mathbf{p})$, which is observable and suitable for calculating its theoretical counterpart (dependent on the cosmological model) reads

$$A(\mathbf{p}) = \frac{\sqrt{\Omega_m}}{0.35} \left[\frac{0.35}{h(0.35; \mathbf{p})} \left(\int_0^{0.35} \frac{dz}{h(z; \mathbf{p})} \right)^2 \right]^{1/3}$$

and the corresponding chi-square is

$$\chi_{\text{BAO}}^2 = \frac{[A(\mathbf{p}) - 0.493]^2}{0.017^2}.$$

2.2 Standard Candles

For more than a decade now, supernovae Ia have been used as standard candles in cosmology. We will use the data set with $n = 557$ supernovae coming from the most recent compilation of SNIa data given in (Amanullah et al. 2010) known as Union2.

The Union2 data set contains redshifts z_i and distance moduli μ_i together with their errors σ_i . This leads to the chi-square function

$$\chi_{\text{SNIa}}^2 = \sum_{i=1}^{N=557} \left[\frac{\mu^{\text{obs}}(z_i) - \mu^{\text{th}}(z_i; \mathbf{p})}{\sigma_i} \right]^2. \quad (8)$$

The distance modulus $\mu := m - M = 5 \log_{10}(D_L(z; \mathbf{p})) + 25$ contains (an unimportant) constant term which can be understood by factoring out the Hubble distance scale from the luminosity distance, i.e. $\mu^{\text{th}}(z_i; \mathbf{p}) = 5 \log_{10}(d_L(z; \mathbf{p})) + \mu_0$, where $\mu_0 = 5 \log_{10}(cH_0^{-1}) + 25$. For the purpose of our analysis, μ_0 is a nuisance parameter. Therefore instead of minimizing the original chi-square in Equation (8), we used an approach equivalent to marginalization over the nuisance parameter, i.e. we minimized the slightly modified expression for χ_{SNIa}^2 as described in Nesseris & Perivolaropoulos (2005). The idea here is to write the chi-square function in Equation (8) as a function of μ_0

$$\chi_{\text{SNIa}}^2 = A - 2\mu_0 B + \mu_0^2 C,$$

where

$$A = \sum_{i=1}^{N=557} \left[\frac{\mu^{\text{obs}}(z_i) - \mu^{\text{th}}(z_i; \mathbf{p}, \mu_0 = 0)}{\sigma_i} \right]^2,$$

$$B = \sum_{i=1}^{N=557} \frac{\mu^{\text{obs}}(z_i) - \mu^{\text{th}}(z_i; \mathbf{p}, \mu_0 = 0)}{\sigma_i},$$

and

$$C = \sum_{i=1}^{N=557} \sigma_i^{-2}.$$

One can see that this is a quadratic function having a minimum value of $\chi_{\text{SNIa},\text{min}}^2 = A - B^2/C$ at $\mu_0 = B/C$. Hence we used such a chi-square minimized over μ_0 . This procedure is equivalent to marginalizing over H_0 as a nuisance parameter. Let us remark here that our diagnostics of standard rulers are independent of H_0 as they can be verified by simple algebra from the respective formulae. Marginalization over H_0 in standard candles makes our joint analysis free from prior assumptions on the value of the Hubble constant.

2.3 Joint Analysis

Standard rulers and standard candles, more precisely – the probes described above – were combined by calculating joint likelihoods

$$\mathcal{L}_{\text{tot}} = \mathcal{L}_{\text{rul}} \times \mathcal{L}_{\text{cand}} = \mathcal{L}_{\text{CMB}} \times \mathcal{L}_{\text{BAO}} \times \mathcal{L}_{\text{Lens}} \times \mathcal{L}_{\text{SNIa}},$$

which is equivalent to the assessment of

$$\chi_{\text{tot}}^2(\mathbf{p}) = \chi_{\text{rul}}^2(\mathbf{p}) + \chi_{\text{cand}}^2(\mathbf{p}) = \chi_{\text{CMB}}^2(\mathbf{p}) + \chi_{\text{BAO}}^2(\mathbf{p}) + \chi_{\text{Lens}}^2(\mathbf{p}) + \chi_{\text{SNIa}}^2(\mathbf{p}).$$

Because standard rulers and standard candles probe distance measures based on different concepts (angular diameter distance and luminosity distance), one step before making a full joint fit was that we performed fits based on rulers and candles separately.

3 COSMOLOGICAL MODELS TESTED AND RESULTS

3.1 Λ CDM and Quintessence Models

The Λ CDM model is a Friedman - Robertson - Walker cosmology with non-vanishing cosmological constant and pressureless matter including the dark matter component responsible for flat rotation curves of galaxies. It is a standard reference point in modern cosmology and is also called the concordance model since it fits rather well with independent data (such as CMBR data, Large Scale Structure considerations, and supernovae data).

There are several reasons why we are not fully satisfied with the concordance scenario. First, the cosmological constant suffers from the fine tuning problem: being constant, why does it start dominating at the present epoch? Then if we imagine its origin as the quantum-mechanical energy of the vacuum, field theoretical estimates predict its value to be 120 orders of magnitude larger than what is observed — currently the biggest discrepancy of theoretical physics (Weinberg 1989).

Hence, another popular explanation of the accelerating Universe is to assume the existence of a negative pressure component called dark energy. One can heuristically assume that this component is described by a hydrodynamical energy-momentum tensor with (effective) cosmic equation of state $p = w\rho$ where $-1 < w < -1/3$. In such a case, this component is called “quintessence.” One can treat the cosmological constant as one possible explanation of dark energy, but since Λ has its own history in General Relativity and cosmology which is independent of the accelerating expansion puzzle, we consider it separately.

Usually, the quintessence is attributed to some sort of a scalar field and the only other scalar field invoked by cosmologists, i.e. the inflaton, clearly had its own dynamics, since the inflationary epoch ended. If we think that the quintessence has its origins in the evolving scalar field, it would be natural to expect that the w coefficient should vary in time, i.e. $w = w(z)$. An arbitrary function $w(z)$ can be Taylor expanded. Then, bearing in mind that both SNIa surveys and strong gravitational lensing

Table 1 Expansion Rates $H(z)$ in the Models Tested

Model	Cosmological expansion rate $H(z)$ (the Hubble function)
Λ CDM	$H^2(z) = H_0^2 [\Omega_m (1+z)^3 + \Omega_\Lambda]$
Quintessence	$H^2(z) = H_0^2 [\Omega_m (1+z)^3 + \Omega_Q (1+z)^{3(1+w)}]$
Chevalier-Polarski-Linder	$H^2(z) = H_0^2 [\Omega_m (1+z)^3 + \Omega_Q (1+z)^{3(1+w_0+w_a)} \exp(\frac{-3w_a z}{1+z})]$
Chaplygin Gas	$H(z)^2 = H_0^2 [\Omega_m(1+z)^3 + \Omega_{Ch}(A_0 + (1 - A_0)(1+z)^{3(1+\alpha)})^{\frac{1}{1+\alpha}}]$
Braneworld	$H(z)^2 = H_0^2 [(\sqrt{\Omega_m}(1+z)^3 + \Omega_{rc} + \sqrt{\Omega_{rc}})^2]$

Notes: The quantities Ω_i represent fractions of critical density currently contained in energy densities of respective components (like clumped pressureless matter, Λ , quintessence, Chaplygin gas or brane effects).

Table 2 Fits to different cosmological models from combined standard ruler data (R+BAO+Lenses).

Cosmological model	Best fit parameters	χ^2
Λ CDM	$\Omega_m = 0.273 \pm 0.018$	63.961
Quintessence	$\Omega_m = 0.262 \pm 0.035$ $w = -1.066 \pm 0.188$	63.829
Chevalier-Polarski-Linder	$\Omega_m = 0.276 \pm 0.055$ $w_0 = -0.824 \pm 0.704$ $w_a = -0.757 \pm 2.148$	63.707
Chaplygin Gas	$\Omega_m = 0.273 \pm 0.018$ $A = 1.000 \pm 0.001$ $\alpha = -0.040 \pm 2.260$	63.961
Braneworld	$\Omega_m = 0.345 \pm 0.021$	72.697

Table 3 Fits to different cosmological models from the Union2 sample of $n = 557$ SNIa.

Cosmological model	Best fit parameters	χ^2
Λ CDM	$\Omega_m = 0.275 \pm 0.020$	663.641
Quintessence	$\Omega_m = 0.299 \pm 0.075$ $w = -1.070 \pm 0.215$	663.532
Chevalier-Polarski-Linder	$\Omega_m = 0.228 \pm 0.156$ $w_0 = -0.993 \pm 0.207$ $w_a = 0.609 \pm 1.071$	663.695
Chaplygin Gas	$\Omega_m = 0.275 \pm 0.020$ $A = 0.999 \pm 0.004$ $\alpha = 0.006 \pm 0.372$	663.641
Braneworld	$\Omega_m = 0.177 \pm 0.015$	664.276

systems are able to probe the range of small to moderate redshifts, it is sufficient to first explore the linear order of this expansion. In earlier literature, the truncated Taylor expansion $w(z) = w_0 + w_1 z$ was used. However, bearing in mind that the scale factor $a(t)$ is a real physical degree of freedom, unlike the redshift z ; the parametrization of $w(z) = w_0 + w_a \frac{z}{1+z}$ developed by Chevallier & Polarski (2001) and Linder (2003) turned out to be well suited and robust for such a case. Therefore, we adopt it as a phenomenological description of the evolving equation of state.

Expansion rates $H(z)$ for cosmological models tested are given in Table 1. Table 2 contains the results for combined standard rulers (Lenses+BAO+CMB) and standard candle results are given in Table 3, whereas Table 4 contains the results of the full joint analysis (Lenses+BAO+CMB+SNIa).

Table 4 Joint R + BAO + Lens + Union2 Fits to Different Cosmological Models.

Cosmological model	Best fit parameters	χ^2
Λ CDM	$\Omega_m = 0.274 \pm 0.014$	727.610
Quintessence	$\Omega_m = 0.274 \pm 0.014$ $w = -1.004 \pm 0.048$	727.603
Chevalier-Polarski-Linder	$\Omega_m = 0.274 \pm 0.014$ $w_0 = -0.989 \pm 0.124$ $w_a = -0.082 \pm 0.621$	727.584
Chaplygin Gas	$\Omega_m = 0.274 \pm 0.014$ $A = 1.0 \pm 0.004$ $\alpha = -0.112 \pm 1.282$	727.610
Braneworld	$\Omega_m = 0.267 \pm 0.013$	777.676

In flat Λ CDM cosmology, Ω_m is the only free parameter. Of course, H_0 is better constrained by other methods. Neither of our standard ruler diagnostics needed the explicit numerical value of H_0 and the standard candle fitting procedure was equivalent to marginalizing over H_0 . The result of our combined analysis, $\Omega_m = 0.274 \pm 0.014$ (see Table 4), should be compared with independent measurements.

The only method sensitive exclusively to matter density comes from studying peculiar velocities of galaxies. The analysis of Feldman et al. (2003) gave $\Omega_m = 0.30^{+0.17}_{-0.07}$ which agrees with our joint analysis within the 1σ range around the central value. Later, Mohayaee & Tully (2005) applied orbit retracing methods to motions in the local supercluster and obtained $\Omega_m = 0.22 \pm 0.02$, which is also consistent with our findings.

In the class of quintessence models, the ESSENCE supernova survey team (Wood-Vasey et al. 2007) pinned down the equation of state parameter to the range $w = -1.07 \pm 0.09(\text{stat}) \pm 0.12$ (systematics) and $\Omega_m = 0.274^{+0.033}_{-0.020}$ (stat 1σ). More recent estimates of $\Omega_m = 0.274^{+0.016+0.013}_{-0.016-0.012}$ and $w = -0.969^{+0.059}_{-0.063}$ (stat) $^{+0.063}_{-0.066}$ (systematics) come from the Union1 SNIa compilation (Kowalski et al. 2008) and from Kessler et al. (2009): $\Omega_m = 0.265 \pm 0.16 \pm 0.025$ and $w = -0.96 \pm 0.06 \pm 0.12$. These results are in perfect agreement with our results shown in Tables 2–4. Confidence regions (corresponding to 68% and 95% confidence limits) in the (Ω_m, w) parameter plane for standard rulers, standard candles and the combined analysis are shown in Figure 1. One can see the different (almost orthogonal) degeneracies of different techniques resulting in a higher restrictive power of combined analysis.

As far as the Chevalier-Polarski-Linder parametrization is concerned, the joint constraint from WMAP+BAO+ H_0 +SN provided by Komatsu et al. (2011) gives the bound $w_0 = -0.93 \pm 0.13$, $w_a = -0.41^{+0.72}_{-0.71}$. The earlier comprehensive analysis of Davis et al. (2007) yielded the best-fit parameter values: $\Omega_m = 0.27 \pm 0.04$, $w_0 = -1.1^{+0.4}_{-0.3}$ and $w_a = 0.8^{+0.8}_{-2.4}$. Our combined analysis gives support to the models with a varying equation of state (in Chevalier-Polarski-Linder parametrization) very close to the Λ CDM model. Respective confidence regions (corresponding to 68% and 95% confidence limits) for standard rulers, standard candles and combined data are shown in Figure 2.

3.2 Generalized Chaplygin Gas Models

In the class of generalized Chaplygin gas models, the matter content of the Universe consists of pressureless gas with energy density ρ_m representing baryonic plus cold dark matter (CDM) and of the generalized Chaplygin gas with the equation of state $p_{\text{Ch}} = -\frac{A}{\rho_{\text{Ch}}^\alpha}$ representing dark energy responsible for the acceleration of the Universe. The original Chaplygin gas corresponds to $\alpha = 1$. In a cosmological context, it has been promoted to the role of a free parameter using a phenom-

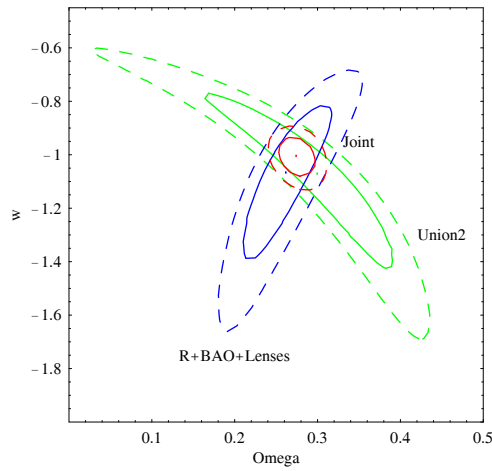


Fig. 1 Best fits (dots) and (68%, 95%) confidence regions in the (Ω, w) plane for the quintessence model. Confidence regions are displayed separately for standard rulers, standard candles and joint analysis.

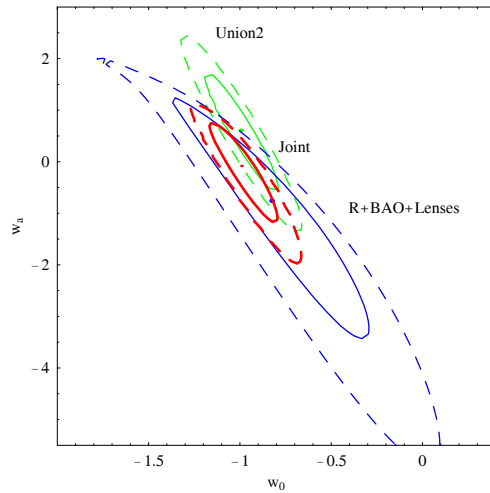


Fig. 2 Best fits (dots) and (68%, 95%) confidence regions in the (w_0, w_a) plane for the Chevalier-Linder-Polarski model. Confidence regions are displayed separately for standard rulers, standard candles and the joint analysis.

logical approach. Values of the α exponent close to zero mean that the model is equivalent to the Λ CDM case.

This exotic form of the cosmic equation of state is inspired by some super-string theories, but at the phenomenological level it has an advantage in that it smoothly interpolates the expansion history of the Universe from matter dominated to dark energy dominated regimes. Chaplygin models have been confronted with different cosmological data like supernovae (Biesiada et al. 2005), cosmic microwave background radiation anisotropies (Amendola et al. 2003), BAO (Wu & Yu 2007), the

integrated Sachs-Wolfe effect (Giannantonio & Melchiorri 2006), X-ray data (Cunha et al. 2004) and age estimates of high- z objects (Alcaniz et al. 2003).

From Tables 2–4, one can see that standard candles and standard rulers consistently support values of α close to zero (and $A \approx 1$). This is in agreement with previous, independent fits (e.g. Biesiada 2006) including the most recent ones (Wu & Yu 2007). Note that a negative central value of the α fit in joint analysis, similar to that reported in Wu & Yu (2007) and in a recent paper by Freitas et al. (2010) (based on the GRB Hubble diagram), is fully compatible with the $\alpha = 0$ case when the confidence intervals are considered. Therefore, we can say that our combined analysis constrains the generalized Chaplygin gas scenario to cases effectively equivalent to the Λ CDM model.

3.3 Brane-world Scenario

Finally, the brane-world models belong to the class of theories which seek the solution that describes the presently accelerating expansion of the Universe, not using an exotic material scheme, but in modifications of gravity. Brane-world scenarios assume that our four-dimensional spacetime is embedded in 5-dimensional space and gravity in 5-dimensions is governed by the usual 5-dimensional Einstein-Hilbert action. The bulk metric induces a 4-dimensional metric on the brane. The brane induced gravity models (Dvali et al. 2000; Dvali & Gabadadze 2001) have a 4-dimensional Einstein-Hilbert action on the brane calculated with the induced metric. According to this picture, our 4-dimensional Universe is a surface (a brane) embedded in a higher dimensional bulk space-time in which gravity propagates. Therefore, there exists a certain cross-over scale r_c above which an observer will detect higher dimensional effects.

As a consequence of modified gravity, the Friedman equation reads

$$H^2 + \frac{k}{a^2} = \left[\sqrt{\frac{\rho}{3M_{Pl}^2} + \frac{1}{4r_c^2}} + \frac{1}{2r_c} \right]^2$$

from which the expansion rate function shown in Table 1 can be derived in the flat ($k = 0$) case. In a flat brane-world Universe, the following relation is also valid: $\Omega_{r_c} = \frac{1}{4}(1 - \Omega_m)^2$. Cosmological models in brane-world scenarios have been widely discussed in the literature (Jain et al. 2002; Alcaniz et al. 2002).

Further research performed in Fairbairn & Goobar (2006) based on the Supernova Legacy Survey combined with SDSS disfavored flat brane-world models. Later analysis by the same authors (Rydbeck et al. 2007) also using the ESSENCE supernovae sample and CMB acoustic peaks lead to the conclusion that the flat brane-world scenario is only slightly disfavored, although inclusion of the baryon acoustic oscillation peak would rule it out. A quite recent paper by Xu & Wang (2010) presents one of the most comprehensive analyses of brane-world models by jointly considering the data from supernovae, gamma-ray bursts, BAO, and CMB peaks, as well as the look back times and growth functions for the large scale structure. Their results (posterior probability distributions for model parameters), obtained by using a Markov Chain Monte Carlo simulation, yield $\Omega_m = 0.266_{-0.0304}^{+0.0298}$ which agrees perfectly with our results of joint analysis reported in Table 3. Let us note that their global best fit for the Λ CDM model, $\Omega_m = 0.274_{-0.0253}^{+0.0323}$, also agrees with our joint analysis results.

4 WHICH MODEL IS THE BEST?

In the previous section, we discussed the best fits of several alternative models to the combined data from standard rulers and standard candles. Such an approach does not say much about the degree of support given to a particular model by the data in comparison with other models. Indeed, each one of the five analyzed models with parameters \mathbf{p} were derived by minimizing the best joint chi-square fits to the data. Minimizing the chi-square is good for finding the best parameters in a model,

but it is insufficient for deciding whether the model itself is the best one. Comparing the models in terms of chi-square values at the best fit or by calculating chi-square per degree of freedom does not account for the relative structural complexity of the models. The sort of questions we raise here can be answered with model selection techniques. Such an approach has already been used in cosmology, see e.g. Liddle (2004, 2007); Liddle et al. (2006); Biesiada (2007); Davis et al. (2007) and references therein and steadily gains popularity. Besides the fully Bayesian model selection techniques based on calculating the Bayesian evidence pursued actively in Kunz et al. (2006); Trotta (2007, 2008), there are two information-theoretic criteria: the Akaike Information Criterion (AIC) and Bayesian Information Criterion (BIC) due to Schwarz.

The Akaike criterion is based on Kullback-Leibler (K-L) information $I(f, g)$ between two distributions $f(x)$ and $g(x)$. The intuitive meaning of $I(f, g)$ (also called K-L divergence) is the information lost when g is used to approximate f . It is convenient to think that $f(x)$ denotes the true mechanism behind the data and $g(x|\mathbf{p})$ is its approximating model (parameterized by \mathbf{p}). Of course, the K-L divergence cannot be assessed without prior knowledge of the true model $f(x)$ as well as parameters \mathbf{p} of the approximating model $g(x|\mathbf{p})$. However, for a given $g(x|\mathbf{p})$, the maximum likelihood estimator $\hat{\mathbf{p}}$ of \mathbf{p} parameters minimizes the K-L divergence.

As was shown by Akaike (1974), the quantity called Akaike Information Criterion

$$\text{AIC} = -2 \ln(\mathcal{L}(\hat{\mathbf{p}}|\text{data})) + 2K \quad (9)$$

is an approximately unbiased estimator of the K-L divergence between the model at hand $g(x|\mathbf{p})$ and an unknown true model $f(x)$ which generated the data. In our case,

$$\text{AIC} = \chi^2(\hat{\mathbf{p}}|\text{data}) + 2K. \quad (10)$$

The AIC value for a single model is meaningless (simply because the true model $f(x)$ is unknown). What is useful instead are the differences $\Delta_i := \text{AIC}_i - \text{AIC}_{\min}$ calculated over the whole set of alternative candidate models $i = 1, \dots, N$ where by AIC_{\min} we denote $\min\{\text{AIC}_i; i = 1, \dots, N\}$. Comparing several models, the one which minimizes AIC could be considered the best. The relative strength of evidence for each model can be calculated as the likelihood of the model given the data $\mathcal{L}(g_i|\text{data}) \propto \exp(-\frac{1}{2}\Delta_i)$. Relative likelihoods of the models $\mathcal{L}(g_i|\text{data})$ normalized to unity are called Akaike weights w_i . In Bayesian language, an Akaike weight corresponds to the posterior probability of a model (under the assumption of equal prior probabilities). The (relative) evidence for the models can also be judged by the evidence ratios of model pairs $\frac{w_i}{w_j} = \frac{\mathcal{L}(g_i|\text{data})}{\mathcal{L}(g_j|\text{data})}$. We will substantiate the evidence ratios as odds against the given model with respect to the best one.

A very similar criterion was derived by Schwarz (1978) in a Bayesian context. It is the so-called Bayesian Information Criterion (BIC)

$$\text{BIC} = -2 \ln(\mathcal{L}(\hat{\mathbf{p}}|\text{data})) + K \ln(n), \quad (11)$$

where n is sample size and, like in the previous case, K denotes the number of parameters. BIC is not an estimator of the K-L divergence; its derivation stems from estimating the marginal likelihood of the data (marginalized over parameters). BIC does not take full advantage of the ability offered by Bayesian techniques.

Tables 5 and 6 contain the AIC and BIC differences, weights and the odds of each of the models against the best one. For the sake of transparency, the odds have been rounded to integer numbers. One can see that the Λ CDM model is the most supported one in light of the joint analysis of standard rulers and standard candles. The Akaike criterion implies that the support given by the data to the quintessential model, even though it is less, is comparable to the concordance model. According to the BIC criterion, the evidence against quintessence is strong. A variable equation of state model and Chaplygin gas scenario, according to AIC, receive similar support but with the evidence against them assessed as moderate. The judgement of BIC is very strongly against these models. Finally, the brane world scenario (DGP model) should be definitely ruled out according to both criteria.

Table 5 AIC Model Selection Results

Model	AIC	Δ_i	w_i	Odds against
Λ CDM	729.610	0.0	0.609	1.0
Quintessence	731.603	1.993	0.225	3.0
Chevalier-Polarski-Linder	733.584	3.974	0.084	7.0
Chaplygin	733.610	4.00	0.082	7.0
Braneworld	779.676	50.066	8.2×10^{-12}	7.0×10^{10}

Notes: Values of AIC, Akaike differences, Akaike weights w_i (in Bayesian language equivalent to posterior model probabilities) and odds against the model (with respect to the best fitted one). Results from the joint analysis of standard rulers and standard candles.

Table 6 BIC Model Selection Results

Model	BIC	BIC Δ_i	BIC w_i	BIC Odds against
Λ CDM	733.97	0.0	0.957	1.0
Quintessence	740.322	6.353	0.040	24.0
Chevalier-Polarski-Linder	746.663	12.693	0.002	570.0
Chaplygin	746.689	12.719	0.002	578.0
Braneworld	784.036	50.066	1.3×10^{-11}	7.0×10^{10}

Notes: Analogous values of Bayesian Information Criterion (BIC); results from joint analysis of standard rulers and standard candles.

5 CONCLUSIONS

In this paper, we performed a joint analysis of five cosmological models invoked to explain the accelerating expansion of the Universe. We used the data from strong gravitational lensing systems, as well as CMB acoustic peak location and BAO data in combination with supernova Ia data (Union2 compilation). The probes we used came from both standard rulers and standard candles. They invoke different (although theoretically related) concepts of a distance in cosmology, hence they have different parameter degeneracies and different restrictive powers in the parameter spaces of cosmological models. The results can best be seen in Figures 2 and 3. This difference (in parameter degeneracy) is responsible for differences in central values of the best fitted cosmological parameters between standard rulers and standard candles.

The best fits we obtained for the model parameters in the joint analysis turned out to be in agreement with other joint analyses performed by others on different sets of diagnostic probes. This illustrates that the power of modern cosmology lies in building up consistency rather than in single, precise, crucial experiments.

Information theoretic methods used to assess which model is the most supported by data lead to the conclusion that the concordance model Λ CDM is preferred and the brane world scenario is practically irrelevant. According to the Akaike criterion, Λ CDM is only slightly preferred over the quintessence case and both models with a dynamical equation of state $w(z)$ (CPL parametrization) and the Chaplygin gas scenario get considerably less support from the data. Odds against the brane-world scenario are so high that it can be considered ruled out by the data. According to the Schwartz Bayesian Information criterion (BIC), Λ CDM wins, the quintessence model is considerably less supported by data and the other ones are ruled out.

Acknowledgements This work was supported by the Polish Ministry of Science Grant No. N N203 390034. The authors would like to thank the referee for his/her creative comments.

References

- Akaike, H. 1974, *IEEE Transactions on Automatic Control*, 19, 716
- Alcaniz, J. S., Jain, D., & Dev, A. 2002, *Phys. Rev. D*, 66, 067301
- Alcaniz, J. S., Jain, D., & Dev, A. 2003, *Phys. Rev. D*, 67, 043514
- Alcock, C., & Paczynski, B. 1979, *Nature*, 281, 358
- Amanullah, R., Lidman, C., Rubin, D., et al. 2010, *ApJ*, 716, 712
- Amendola, L., Finelli, F., Burigana, C., & Carturan, D. 2003, *J. Cosmol. Astropart. Phys.*, 7, 5
- Astier, P., Guy, J., Regnault, N., et al. 2006, *A&A*, 447, 31
- Biesiada, M. 2006, *Phys. Rev. D*, 73, 023006
- Biesiada, M. 2007, *J. Cosmol. Astropart. Phys.*, 2, 3
- Biesiada, M., Godłowski, W., & Szydlowski, M. 2005, *ApJ*, 622, 28
- Biesiada, M., Piórkowska, A., & Malec, B. 2010, *MNRAS*, 406, 1055
- Chevallier, M., & Polarski, D. 2001, *International Journal of Modern Physics D*, 10, 213
- Cole, S., Percival, W. J., Peacock, J. A., et al. 2005, *MNRAS*, 362, 505
- Cunha, J. V., Alcaniz, J. S., & Lima, J. A. 2004, *Phys. Rev. D*, 69, 083501
- Davis, T. M., Mörtzell, E., Sollerman, J., et al. 2007, *ApJ*, 666, 716
- Doran, M., & Lilley, M. 2002, *MNRAS*, 330, 965
- Dvali, G., & Gabadadze, G. 2001, *Phys. Rev. D*, 63, 065007
- Dvali, G., Gabadadze, G., & Porrati, M. 2000, *Physics Letters B*, 485, 208
- Eisenstein, D. J., & Hu, W. 1999, *ApJ*, 511, 5
- Eisenstein, D. J., Zehavi, I., Hogg, D. W., et al. 2005, *ApJ*, 633, 560
- Fairbairn, M., & Goobar, A. 2006, *Physics Letters B*, 642, 432
- Feldman, H., Juszkwicz, R., Ferreira, P., et al. 2003, *ApJ*, 596, L131
- Freitas, R. C., Gonçalves, S. V. B., & Velten, H. E. S. 2010, arXiv:1004.5585
- Giannantonio, T., & Melchiorri, A. 2006, *Classical and Quantum Gravity*, 23, 4125
- Grillo, C., Lombardi, M., & Bertin, G. 2008, *A&A*, 477, 397
- Hicken, M., Wood-Vasey, W. M., Blondin, S., et al. 2009, *ApJ*, 700, 1097
- Hinshaw, G., Weiland, J. L., Hill, R. S., et al. 2009, *ApJS*, 180, 225
- Hütsi, G. 2006a, *A&A*, 449, 891
- Hütsi, G. 2006b, *A&A*, 459, 375
- Jain, D., Dev, A., & Alcaniz, J. S. 2002, *Phys. Rev. D*, 66, 083511
- Kessler, R., Becker, A. C., Cinabro, D., et al. 2009, *ApJS*, 185, 32
- Komatsu, E., Dunkley, J., Nolta, M. R., et al. 2009, *ApJS*, 180, 330
- Komatsu, E., Smith, K. M., Dunkley, J., et al. 2011, *ApJS*, 192, 18
- Koopmans, L. V. E., Bolton, A., Treu, T., et al. 2009, *ApJ*, 703, L51
- Koopmans, L. V. E., & Treu, T. 2002, *ApJ*, 568, L5
- Koopmans, L. V. E., & Treu, T. 2003, *ApJ*, 583, 606
- Koopmans, L. V. E., Treu, T., Bolton, A. S., Burles, S., & Moustakas, L. A. 2006, *ApJ*, 649, 599
- Kowalski, M., Rubin, D., Aldering, G., et al. 2008, *ApJ*, 686, 749
- Kunz, M., Trotta, R., & Parkinson, D. R. 2006, *Phys. Rev. D*, 74, 023503
- Liddle, A. R. 2004, *MNRAS*, 351, L49
- Liddle, A. R. 2007, *MNRAS*, 377, L74
- Liddle, A. R., Mukherjee, P., Parkinson, D., & Wang, Y. 2006, *Phys. Rev. D*, 74, 123506
- Linder, E. V. 2003, *Phys. Rev. D*, 68, 083503
- Mohayaee, R., & Tully, R. B. 2005, *ApJ*, 635, L113
- Nesseris, S., & Perivolaropoulos, L. 2005, *Phys. Rev. D*, 72, 123519
- Page, L., Nolta, M. R., Barnes, C., et al. 2003, *ApJS*, 148, 233
- Percival, W. J., Nichol, R. C., Eisenstein, D. J., et al. 2007, *ApJ*, 657, 51

- Perlmutter, S., Aldering, G., Goldhaber, G., et al. 1999, *ApJ*, 517, 565
- Reid, B. A., Percival, W. J., Eisenstein, D. J., et al. 2010, *MNRAS*, 404, 60
- Riess, A. G., Filippenko, A. V., Challis, P., et al. 1998, *AJ*, 116, 1009
- Riess, A. G., Strolger, L., Casertano, S., et al. 2007, *ApJ*, 659, 98
- Riess, A. G., Strolger, L., Tonry, J., et al. 2004, *ApJ*, 607, 665
- Rydbeck, S., Fairbairn, M., & Goobar, A. 2007, *J. Cosmol. Astropart. Phys.*, 5, 3
- Schwarz, G. 1978, *The Annals of Statistics*, 6, 461
- Shafieloo, A., Sahni, V., & Starobinsky, A. A. 2009, *Phys. Rev. D*, 80, 101301
- Spergel, D. N., Bean, R., Doré, O., et al. 2007, *ApJS*, 170, 377
- Treu, T., Koopmans, L. V., Bolton, A. S., Burles, S., & Moustakas, L. A. 2006a, *ApJ*, 640, 662
- Treu, T., & Koopmans, L. V. E. 2004, *ApJ*, 611, 739
- Treu, T., Koopmans, L. V. E., Bolton, A. S., Burles, S., & Moustakas, L. A. 2006b, *ApJ*, 650, 1219
- Trotta, R. 2007, *MNRAS*, 378, 819
- Trotta, R. 2008, *Contemporary Physics*, 49, 71
- Weinberg, S. 1989, *Reviews of Modern Physics*, 61, 1
- Wood-Vasey, W. M., Miknaitis, G., Stubbs, C. W., et al. 2007, *ApJ*, 666, 694
- Wu, P., & Yu, H. 2007, *ApJ*, 658, 663
- Xu, L., & Wang, Y. 2010, *Phys. Rev. D*, 82, 043503